Available online at www.sciencedirect.com
SCIENCE DIRECT®
Journal of Solid State Chemistry 178 (2005) 2907–2912
JOURNAL OF SOLID STATE CHEMISTRY
www.elsevier.com/locate/jssc

Defect structure of $Sb_{2-x}Mn_xTe_3$ single crystals

Jaromír Horák[a], Petr Lošťák[b], Čestmír Drašar[b,*], Jeffrey S. Dyck[c,1], Zengzua Zhou[c], Ctirad Uher[c]

[a]Joint Laboratory of Solid State Chemistry of Institute of Macromolecular Chemistry of the Academy of Sciences of the Czech Republic and University of Pardubice, Studentská 84, 532 10 Pardubice, Czech Republic
[b]Faculty of Chemical Technology, University of Pardubice, Cs. Legii Square 565, 532 10 Pardubice, Czech Republic
[c]Department of Physics, University of Michigan, Ann Arbor, MI 48109-1120, USA

Received 14 March 2005; received in revised form 14 June 2005; accepted 20 June 2005

Abstract

Incorporation of the transition metal elements in the tetradymite structure of Sb_2Te_3 has a strong influence on electronic properties. Recent studies have indicated that Mn substitutes on the Sb sublattice increases the carrier concentration of holes. However, the doping efficiency of Mn appears rather low in comparison to what it should be based on the measurements of magnetization, structural analysis, and transport properties. In this paper we address this issue by making detailed studies of the Hall effect and electrical resistivity and we explain the results with the aid of a model that takes into account interactions of the Mn impurity with the native defects in antimony telluride. Specifically, we find that Mn atoms interact with antisite defects (antimony atoms located on the tellurium sublattice), a process that decreases the density of antisite centers and generates free electrons. These, in turn, recombine with holes and thus decrease their concentration and the apparent Mn doping efficiency.

Keywords: Point defects; Transport properties; $Sb_{2-x}Mn_xTe_3$

1. Introduction

Recent studies probing the influence of transition metal impurities on the electronic structure and transport parameters of the tetradymite-type crystals with the space group $D^5_{3d} - R\bar{3}m$ (Sb_2Te_3, Bi_2Te_3) have resulted in unexpected findings. Among the most surprising results was the discovery that certain $3d$ impurities stimulate a long-range ferromagnetic order, i.e., some of these compounds are diluted magnetic semiconductors [1–3]. Since Mn is an archetypal stimulant of the magnetic order in the intensely pursued III–V diluted magnetic semiconductors [4–6], we decided to explore its influence in the environment of the layered, tetradymite-type matrix. Although the otherwise diamagnetic structure of Sb_2Te_3 displayed a strong paramagnetism upon incorporation of Mn, no long-range magnetic order was detected down to 2 K even for the highest Mn content (corresponding to the formula $Sb_{1.955}Mn_{0.045}Te_3$ [7]). The analysis of the magnetic susceptibility and the Brillouin function indicated that manganese substitutes for Sb and attains the Mn^{+2} state with $S = 5/2$. Nonetheless, the transport characterization of the samples indicated an anomalous doping dependence and a rather low doping efficiency of Mn. We have therefore decided to study these features in detail.

In this paper we present detailed Hall and resistivity measurements made on a series of Mn-doped Sb_2Te_3 single crystals and we describe a model that explains the experimental data based on the interaction of Mn impurity with the native defect structure of Sb_2Te_3 crystals.

*Corresponding author. Fax: +420466036033.
E-mail address: cestmir.drasar@upce.cz (C. Drašar).
[1]Present address: Department of Physics, John Carroll University, University Heights, OH 44118, USA.

0022-4596/$ - see front matter © 2005 Elsevier Inc. All rights reserved.
doi:10.1016/j.jssc.2005.06.026

2. Experimental

Single crystals of $Sb_{2-x}Mn_xTe_3$ (nominal values $x = 0.0-0.06$) were prepared from stoichiometric amounts of the elements of 5 N purity using the Bridgman method as described elsewhere [8]. Samples with the dimensions of $5 \times 2.5 \times 2.5\,mm^3$ were cut out from the middle part of the single crystal ingots. The actual concentration of Mn in the samples was determined using electron microprobe analysis.

The Hall coefficient $R_H(\mathbf{B}\|\mathbf{c})$ and electrical resistivity $\rho_{\perp c}$ were studied using a Linear Research AC bridge with 16 Hz excitation in a magnet cryostat capable of fields up to 5 T. Measurements of these parameters were made over the temperature range of 5–300 K. Figs. 1 and 2 show the temperature dependence of the Hall coefficient $R_H(\mathbf{B}\|\mathbf{c})$ and of the electrical resistivity, respectively, while in Fig. 3 are plotted the concentration dependences of the above two transport parameters. From the experimental values of $R_H(\mathbf{B}\|\mathbf{c})$ and $\rho_{\perp c}$ we calculated the carrier mobility for each sample that is shown in Fig. 4. It is evident that the incorporation of Mn atoms in to the Sb_2Te_3 crystal lattice leads to a decrease of $R_H(\mathbf{B}\|\mathbf{c})$ and $\rho_{\perp c}$ values; the free carrier mobility given by expression $R_H/\rho_{\perp c}$ decreases as well.

To obtain the free carrier density P, we use the expression $R_H(\mathbf{B}\|\mathbf{c}) = \gamma(r_H/Pe)$, where e is the electron charge, γ is the structure factor and r_H is the scattering factor in the Hall constant. For γ we use the value of 0.74, given in Ref. [9], and we assume that the value of γ does not change with the incorporation of manganese into the crystal lattice of Sb_2Te_3. Furthermore, we assume that the scattering factor r_H is equal to unity, i.e., $r_H = 1$. The resulting values of P, obtained this way, are given in Table 1.

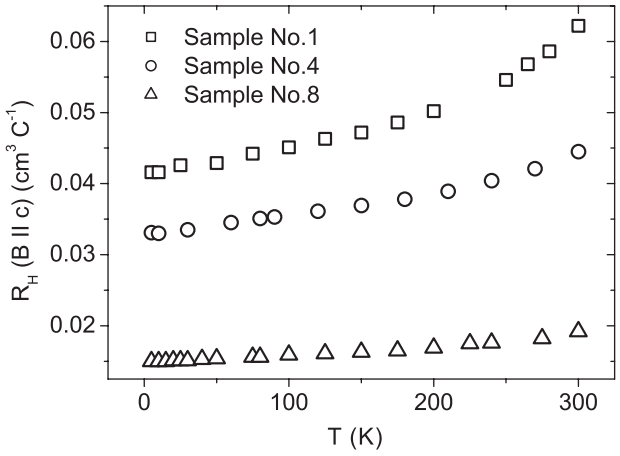

Fig. 1. Temperature dependence of the Hall coefficient $R_H(\mathbf{B}\|\mathbf{c})$ of $Sb_{2-x}Mn_xTe_3$ single crystals (samples are labeled according to Table 1).

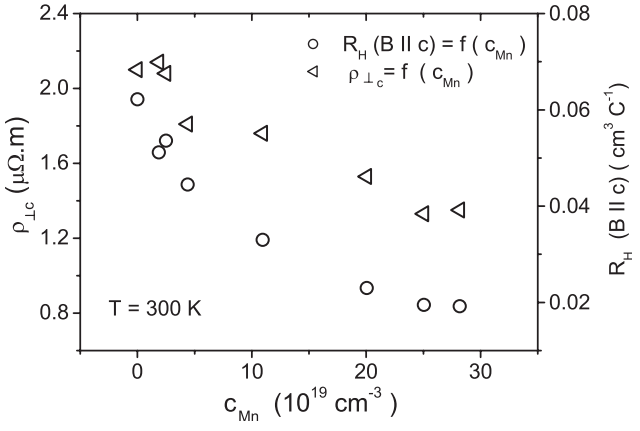

Fig. 3. Hall coefficient $R_H(\mathbf{B}\|\mathbf{c})$ and electrical resistivity $\rho_{\perp c}$ at $T = 300$ K as a function of Mn concentration c_{Mn} for $Sb_{2-x}Mn_xTe_3$ single crystals.

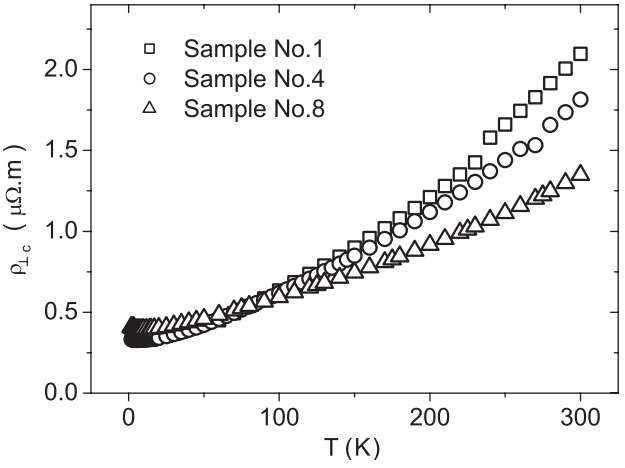

Fig. 2. Temperature dependence of the electrical resistivity $\rho_{\perp c}$ of $Sb_{2-x}Mn_xTe_3$ single crystals (samples are labeled according to Table 1).

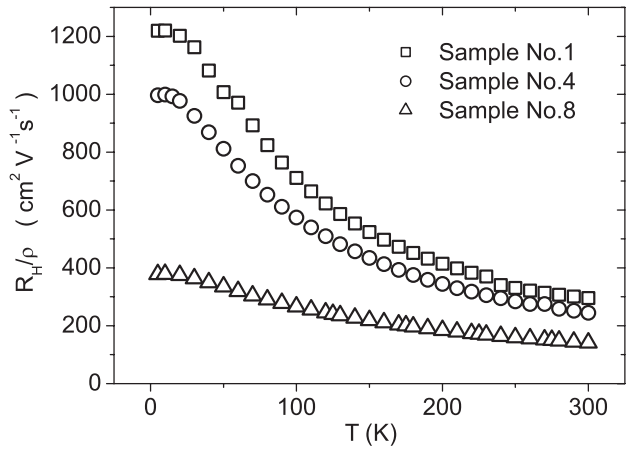

Fig. 4. Hall mobility (R_H/ρ) of holes in single crystals of $Sb_{2-x}Mn_xTe_3$ as a function of temperature (samples are labeled according to Table 1).

Table 1
Room temperature values of Hall coefficient $R_H(\mathbf{B}\|\mathbf{c})$, electrical resistivity $\rho_{\perp c}$, and free-carrier concentration P in $Sb_{2-x}Mn_xTe_3$ crystals as a function of manganese concentration c_{Mn}

Sample no.	c_{Mn} (10^{19} cm^{-3})	$R_H(\mathbf{B}\|\mathbf{c})$ (cm^3/C)	$\rho_{\perp c}$ (μΩm)	P (10^{19} cm^{-3})	ΔP (10^{19} cm^{-3})	$\Delta P/c_{Mn}$ (−)
1	0	0.0622	2.10	7.44	—	—
2	1.88	0.0512	2.14	9.03	1.59	0.84
3	2.50	0.0536	2.08	8.63	1.19	0.51
4	4.38	0.0445	1.81	10.38	2.95	0.67
5	10.96	0.0330	1.76	14.02	6.58	0.60
6	20.04	0.0230	1.53	20.10	12.67	0.63
7	25.04	0.0195	1.33	23.72	16.28	0.65
8	28.17	0.0192	1.35	24.09	16.65	0.59

Changes in the concentration of holes were calculated as $\Delta P = P - P_0$, where P_0 is the concentration of holes in the undoped Sb_2Te_3 crystal. The ratio $\Delta P/c_{Mn}$ (the increase in the concentration of holes due to the incorporation of Mn atoms in the lattice corresponding to 1 incorporated Mn atom) is entered in the last column of Table 1.

3. Discussion

The structure of Sb_2Te_3 crystals is formed by a periodic arrangement of layers situated perpendicular to the trigonal axis (the c-axis). Each layer is composed of five atomic planes arranged according to the following pattern:

$$\ldots Te^1 - Sb - Te^2 - Sb - Te^1$$

$$\ldots Te^1 - Sb - Te^2 - Sb - Te^1 \ldots.$$

Bonding between the neighboring Te^1 atomic planes is weak and is of the van der Waals character [10]. As shown in Ref. [7], the incorporation of Mn atoms into the Sb_2Te_3 crystals results in the paramagnetic behavior of Mn-doped Sb_2Te_3. The effective magnetic moment obtained from the data is 5.8–5.9 μ_B, showing unambiguously that Mn atoms are present in the valence state +2. With regard to the crystal structure, we assume that Mn atoms possess octahedral coordination with Te atoms that occupy the corner octahedra positions. Mn atoms can be located at two positions in the Sb_2Te_3 crystal lattice. The first one is situated in the plane of Sb atoms (between the planes of Te^1 and Te^2), while the second one is in the middle of the empty octahedron inside the van der Waals gap with the apices formed by the Te^1 atoms of the adjacent Te^1 planes. The second location, the one placing Mn atoms in the van der Waals gap, is however very unlikely because such Mn ions would generate free electrons leading to a decrease in the concentration of holes. Moreover, excellent cleavage characteristics of the crystals along the c-axis would be adversely affected by the presence of Mn in the van der Waals gap. As the concentration of holes increases with the increasing Mn content we can assume that Mn atoms are indeed located on the sites of the cation sublattice. Therefore, the incorporation of Mn in the Sb_2Te_3 lattice leads to the formation of substitutional defects Mn'_{Sb}, as proposed originally [11].

Manganese at the positions of the cation sublattice (as Mn'_{Sb} defects), imply the creation of one hole per Mn atom. The experimental data presented in Table 1, however, show an increase in the concentration of holes ΔP that is considerably smaller. Specifically, the ratio $\Delta P/c_{Mn}$ varies within the range of only 0.50–0.84. As we show below, the observed discrepancy between the number of incorporated Mn atoms and the number of holes generated can be explained by interaction processes between the dopant atoms and native defects in the Sb_2Te_3 crystal lattice.

Native defects arise during the crystal growth from melt and their concentration in Sb_2Te_3 is the consequence of the overstoichiometric content of antimony. The excess of Sb in the otherwise stoichiometrically weighted composition (2Sb + 3Te) is associated with a shift of the maximum of the solidus curve in the Sb–Te phase diagram towards the side of Sb [12]. Crystals of Sb_2Te_3 prepared from stoichiometric melts invariably contain the following defects:

(a) vacancies on the Te sublattice that carry 2 positive charges, $V^{\bullet\bullet}_{Te}$,
(b) antisite defects (AS defects) such as Sb atoms on the Te-sublattice that carry one negative charge, Sb'_{Te},
(c) vacancies on the Sb sublattice with 3 negative charges V'''_{Sb} [13],
(d) structural defects such as $Sb_3Te'_4$, $Sb_4Te''_5$ (seven- and nine-layer lamellas observed in Ref. [14] that mimic the charge contribution of one, respectively, two antisite defects Sb'_{Te}).

To calculate the concentration of antisite defects Sb'_{Te} and vacancies V'''_{Sb} and $V^{\bullet\bullet}_{Te}$ we use a simple model based on the idea that only a certain part of the total overstoichiometric antimony content Sb_{over} is

incorporated in the antimony sublattice (denoted Sb_{Sb}) and the remaining part enters the Te sublattice forming antisite defects Sb'_{Te2} (that means that the antisite defects are created in Te^2 atomic planes). Considerable understoichiometry of Te (as the chemical analysis shows) gives rise to tellurium vacancies $V^{\bullet\bullet}_{Te}$. Since it is not possible to determine, from the transport measurements, if $V^{\bullet\bullet}_{Te}$ vacancies are created in the Te^1-, or Te^2- atomic planes we have assumed that the vacancies $V^{\bullet\bullet}_{Te}$ compensating the negative charge of Sb'_{Te} are concentrated in the Te^1-planes. According to the model, the ratio of cation to anion sites is equal to 2:3. Using these simplifications the incorporation of Sb_{over} can be described by the following equation:

$$a\mathrm{Sb}_{over} + b(V_{Sb} + 1.5\ V_{Te})^{\times} = \mathrm{Sb}_{Sb} + (a-b)\mathrm{Sb}'_{Te} + (5/2.b - a) + (3a - 6b). \quad (1)$$

(The symbol $^{\times}$ means that the sum of charges of given vacances in the parentheses equals to zero; a, and b are stoichiometric coefficients).

Chemical analysis gives the stoichiometry $Sb_2Te_{2.95}$, i.e., $Sb_{over} = 2.12 \times 10^{20}$ Sb-atom cm^{-3}. The hole concentration from Hall measurements is $p = 7.4 \times 10^{19}\,cm^{-3}$. This model is characterized by the following relations:

$$[\mathrm{Sb}_{over}] = [\mathrm{Sb}_{Sb}] + [\mathrm{Sb}'_{Te}], \quad (2a)$$

$$2[V^{\bullet\bullet}_{Te}] + [h^{\bullet}] = [\mathrm{Sb}'_{Te}], \quad (2b)$$

$$[\mathrm{Sb}_{Sb}]/([V^{\bullet\bullet}_{Te}] + [\mathrm{Sb}'_{Te}]) = 2/3. \quad (2c)$$

Calculations based on this model for an undoped $Sb_2Te_{2.95}$ crystal prepared from a stoichiometric melt give the following results:

$[\mathrm{Sb}_{over}] = 2.12 \times 10^{20}\,cm^{-3}$,
$[\mathrm{Sb}_{Sb}] = 9.37 \times 10^{19}\,cm^{-3}$,
$[\mathrm{Sb}'_{Te}] = 11.83 \times 10^{19}\,cm^{-3}$,
$[V^{\bullet\bullet}_{Te}] = 2.225 \times 10^{19}\,cm^{-3}$.

It seems that this model works well for the undoped crystal. However, we have to extend the model by including the existence of antimony vacancies V'''_{Sb} when considering doped crystals. Namely, the reaction usually describing the incorporation of a metal atom in tetradymite crystals requires vacancies (in this case $V'''_{Sb} + Mn^{+2} = Mn'_{Sb}$). Moreover, the reaction relevant to the n- to p-type transition in the tetradymite crystal requires the existence of antimony vacancies:

$$\mathrm{Sb}_{Sb} + V^{\bullet\bullet}_{Te} + 2e' \Leftrightarrow \mathrm{Sb}'_{Te} + V'''_{Sb} + 4h^{\bullet}. \quad (3)$$

Eq. (3) implies that the formation of one antisite defect Sb'_{Te} produces one antimony vacancy V'''_{Sb}. Thus the relations (Eqs. 2(a,b,c)) must be modified as follows:

$$[\mathrm{Sb}_{over}] = [\mathrm{Sb}_{Sb}] + [\mathrm{Sb}'_{Te}], \quad (4a)$$

$$[V'''_{Sb}] = [\mathrm{Sb}'_{Te}], \quad (4b)$$

$$[V^{\bullet\bullet}_{Te}] + [h^{\bullet}] = [\mathrm{Sb}'_{Te}] + 3[V'''_{Sb}], \quad (4c)$$

$$([\mathrm{Sb}_{Sb}] + [V'''_{Sb}])/([V^{\bullet\bullet}_{Te}] + [\mathrm{Sb}'_{Te}]) = 2/3 \quad (4d)$$

Now, the calculations yield the following results:

$[\mathrm{Sb}_{over}] = 2.12 \times 10^{20}\,cm^{-3}$,
$[\mathrm{Sb}_{Sb}] = 9.40 \times 10^{19}\,cm^{-3}$,
$[\mathrm{Sb}'_{Te}] = 11.8 \times 10^{19}\,cm^{-3}$,
$[V'''_{Sb}] = 11.8 \times 10^{19}\,cm^{-3}$,
$[V^{\bullet\bullet}_{Te}] = 19.9 \times 10^{19}\,cm^{-3}$.

Regarding the relation $(2V'''_{Sb} + 3V^{\bullet\bullet}_{Te}) = 0$, the concentration of tellurium vacancies producing two electrons $[V^{\bullet\bullet}_{Te}] \cong 2.2 \times 10^{19}\,cm^{-3}$. Thus the calculated concentrations of $V^{\bullet\bullet}_{Te}$ and Sb'_{Te} is not influenced when we omit the V'''_{Sb}. It shows, however, that whatever interaction we describe we have to cancel one V'''_{Sb} when canceling one Sb'_{Te}, as described below.

The knowledge of the character and the concentration of native defects in non-stoichiometric Sb_2Te_{3-z} allows one to explain the observed small increase in the hole concentration in Mn-doped Sb_2Te_3 crystals in the following way: Manganese atoms entering Sb_2Te_3 crystal structure interact with native defects present in the undoped crystal. Considering the incorporation of Mn atoms into the crystal structure we assume the following limitations:

1. Mn atoms do not enter anion sublattice.
2. According to measurement of magnetic susceptibility [7] Mn atoms are present in their lowest valency $+2$.
3. The small ionic radius of Mn^{2+} (0.080 nm) does not preclude the incorporation of Mn into interstitial positions in the structure. However, such defects would completely suppress the hole concentration. As these defects are not in agreement with the experimental results, we do not consider their formation nor the presence of Mn^{2+} ions in the van der Waals gap.

The above listed constraints result in two most probable ways of incorporation of Mn atoms into the crystal structure of Sb_2Te_3 described by the equations:

$$(2\ V_{Sb} + 3\ V_{Te})^{\times} + 2\mathrm{Mn} + 3\mathrm{Te} = 2\mathrm{Mn}'_{Sb} + 3\mathrm{Te}_{Te} + 2h^{\bullet} \quad (5)$$

$$2\mathrm{Sb}'_{Te} + 2h^{\bullet} + 2(2V_{Sb} + 3V_{Te})^{\times} + 2\mathrm{Mn} + 3\mathrm{Te}_{Te} + 2\mathrm{Mn}'_{Sb} + 5V^{\bullet\bullet}_{Te} + 8e' \quad (6)$$

Table 2
Calculated concentrations of crystal lattice defects in $Sb_{2-x}Mn_xTe_3$ single crystals

Sample no.	$[^1Mn'_{Sb}]$ ($10^{19}cm^{-3}$)	$[^2Mn'_{Sb}]$ ($10^{19}cm^{-3}$)	$[Sb'_{Te}]$ ($10^{19}cm^{-3}$)	$\Delta[V^{\bullet\bullet}_{Te}]^a$ ($10^{19}\,cm^{-3}$)	$[\Delta e']$ ($10^{19}\,cm^{-3}$)
1	0	0	11.80	0	0
2	1.82	0.058	11.742	0.145	0.232
3	2.26	0.262	11.538	0.655	1.048
4	4.10	0.287	11.513	0.716	1.148
5	10.08	0.876	10.924	2.190	3.504
6	18.57	1.474	9.862	3.685	5.846
7	23.29	1.750	10.050	4.375	7.000
8	25.87	2.304	9.496	5.760	9.216

[a]$\Delta[V^{\bullet\bullet}_{Te}] = [V^{\bullet\bullet}_{Te}] - [V^{\bullet\bullet}_{Te}]_0$, where $[V^{\bullet\bullet}_{Te}]_0$ is the concentration of Te vacancies in the undoped crystal.

According to Eqs. (5) and (6), Mn atoms enter positions in the Sb sublattice V'''_{Sb} and interact with AS defects which results in the formation of vacancies $V^{\bullet\bullet}_{Te}$ and electrons. These electrons recombine with free holes thus decreasing their concentration.

If we use the model regarding the presence of V'''_{Sb} in the crystal according to Eqs. (4a–d), we describe the incorporation of Mn atoms by the equation:

$$2(Sb'_{Te} + V'''_{Sb}) + 8h^{\bullet} + (2V_{Sb} + 3V_{Te})^{\times} + (2Mn + 3Te) = (2Sb_{Sb} + 3Te_{Te}) + 2Mn'_{Sb} + 2V^{\bullet\bullet}_{Te} + 2e'. \quad (7)$$

While the nature of incorporation of Mn is the same in both cases, the difference between processes outlined in Eqs. (6) and (7) is in the concentration of $V^{\bullet\bullet}_{Te}$ and the concentration of free electrons generated; both being smaller in the latter case due to suppression of concentration of V'''_{Sb}.

The validity of Eqs. (6) and (7) that describe the incorporation of Mn atoms into the crystal structure of Sb_2Te_3 is also supported by the fact that by subtracting Eq. (5) from Eqs. (6) and (7) we obtain the expression describing the transition between p- and n-type tellurides of tetradymite structure as given by Eq. (2).

The proposed description of the incorporation of Mn-atoms into the Sb_2Te_3 crystal according to Eqs. (6) and (7) helps us to explain the observed discrepancy between the number of incorporated Mn atoms and the observed increase in the concentration of holes. A part of Mn-atoms (denoted as ^1Mn) is incorporated according to Eq. (5)—they enter cation vacancies and form substitutional $^1Mn'_{Sb}$ defects. The remaining Mn atoms (denoted as ^2Mn) interact with antisite defects Sb'_{Te} and decrease their concentration. Sb-atoms leaving the antisite positions in the anion sublattice move into the cation sublattice producing four electrons (see Eq. (6)); the atoms ^2Mn are also incorporated into the cation sublattice forming there substitutional defects Mn'_{Sb} and vacancies $V^{\bullet\bullet}_{Te}$. This consideration results in several

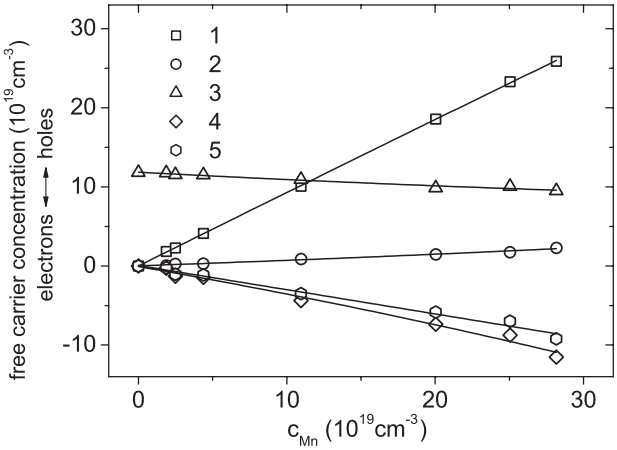

Fig. 5. Free carrier concentration as a function of the content of Mn (c_{Mn}) incorporated in the lattice of Sb_2Te_3. Curve #1: Concentration of holes created by substitutional defects $^1Mn'_{Sb}$. Curve #2: Concentration of holes created by substitutional defects $^2Mn'_{Sb}$. Curve #3: Concentration of holes corresponding to antisite defects Sb'_{Te}. Curve #4: change in the electron concentration compensating the charge of Te-vacancies. Curve #5: electron concentration $[\Delta e']$ produced according to Eq. (6).

simple relations:

$$[^1Mn'_{Sb}] + [^2Mn'_{Sb}] = c_{Mn};$$
$$P(^1Mn'_{Sb}) + P(^2Mn'_{Sb}) = \Delta P. \quad (8a, b)$$

This follows from

$$P(^1Mn'_{Sb}) = [^1Mn], \quad P(^2Mn'_{Sb}) = -4[^2Mn'_{Sb}],$$
$$\text{and} \quad 2[V^{\bullet\bullet}_{Te}] = [\Delta e'] + [^2Mn'_{Sb}], \quad (9)$$

where $[\Delta e']$ is the concentration of free electrons produced by transmigration of Sb atoms from the anion sublattice (antisite defect Sb'_{Te}) into the cation sublattice (regular place).

The concentrations of $[^1Mn'_{Sb}]$ and $[^2Mn'_{Sb}]$ defects were determined from Eqs. (8a,b), and the concentration of $[V^{\bullet\bullet}_{Te}]$ defects from Eqs. (6) and (9). The calculated values of all these defects are summarised in Table 2.

Changes in the concentration of all structural defects with the concentration of incorporated Mn are shown in Fig. 5.

Eq. (7) indicates that the changes in the hole concentration, caused by the incorporation of Mn atoms, are associated with the increase in $[V_{Te}^{\bullet\bullet}]$ and simultaneously with the suppression of the concentration of antisite defects $[Sb'_{Te}]$ and vacancies $[V'''_{Sb}]$. It means that the addition of Mn atoms to Sb_2Te_3 (to prepare crystals of $Sb_{2-x}Mn_xTe_3$) decreases the probability of formation of antisite defects and also of cation vacancies during the growth, whereas the probability of formation of $V_{Te}^{\bullet\bullet}$ defects significantly increases with the increasing c_{Mn}. We should mention here that the maximum concentration of incorporated Mn atoms $c_{Mn} = 28.17 \times 10^{19}\,cm^{-3}$ corresponds to the formula $Sb_{1.955}Mn_{0.045}Te_3$.

These results show that the apparent discrepancy between the concentration of incorporated Mn atoms in Sb_2Te_3 and the observed increase in the concentration of holes can be readily explained in terms of the interaction of doping atoms with antisite defects, the defects that are native to the layered tetradymite-type structure. The formation of substitutional defects Mn'_{Sb} and the considerable increase in the concentration of vacancies $V_{Te}^{\bullet\bullet}$ strongly affect transport properties and the hole mobility in particular (Fig. 4). The pronounced increase in vacancies $V_{Te}^{\bullet\bullet}$ also undoubtedly contributes to a decrease of thermal conductivity of $Sb_{2-x}Mn_xTe_3$ single crystals, as observed recently [15].

4. Conclusions

1. Experimental measurements showed that the incorporation of Mn atoms into Sb_2Te_3 crystals results in an increase in the concentration of holes for all $Sb_{2-x}Mn_xTe_3$ crystals within the range of $x = 0.0$–0.045 studied in this work. The most probable explanation of these changes is the formation of Mn'_{Sb} defects carrying one negative charge and generating one hole. Similar conclusion was made from the measurement of magnetic susceptibility of $Sb_{2-x}Mn_xTe_3$ crystals.
2. The concentration of holes determined from measurements of the Hall coefficient is, however, significantly smaller than the concentration of Mn acceptors incorporated in the crystal lattice ($\Delta P/c_{Mn} \sim 0.50$–$0.84$ over the range of x). Thus, a part of incorporated Mn atoms seems to be electrically inactive. This discrepancy is explained by the interaction of Mn atoms with antisite defects Sb'_{Te}, which takes place during the crystal growth. One part of Mn atoms enters cation sublattice creating Mn'_{Sb} defects accompanied by the formation of holes. The other part of Mn atoms interacts with antisite defects resulting in a decrease in the concentration of Sb'_{Te} defects, which is accompanied by the formation of electrons.
3. The model describing the relationship between the overstoichiometry of Sb and the concentration of native defects in undoped Sb_2Te_3 crystals shows that the suppression of the concentration of Sb'_{Te}defects is associated with a decrease in the concentration of antimony vacancies V'''_{Sb} and an increase in the concentration of tellurium vacancies $V_{Te}^{\bullet\bullet}$.

Acknowledgments

The authors gratefully acknowledge the support of the Ministry of Education of the Czech Republic under the project MSM 002167501, and the National Science Foundation Grants NSF-INT 0201114 and NSF-DMR 0305221.

References

[1] V.A. Kulbachinskii, A. Yu. Kaminskii, K. Kindo, Y. Narumi, K. Suga, P. Lošťák, P. Švanda, JETP Lett. 73 (2001) 352.
[2] J.S. Dyck, P. Hájek, P. Lošťák, C. Uher, Phys. Rev. B 65 (2002) 115212.
[3] J.S. Dyck, Č. Drašar, P. Lošťák, C. Uher, Phys. Rev. B 71 (2005) 115214.
[4] H. Ohno, J. Magn. Magn. Mater. 200 (1999) 110.
[5] T. Dietl, Semicond. Sci. Technol. 17 (2002) 377.
[6] S.J. Pearton, C.R. Abernathy, D.P. Norton, A.F. Hebard, Y.D. Park, L.A. Boatner, J.D. Budai, Mater. Sci. Eng. R. 40 (2003) 137.
[7] J.S. Dyck, P. Švanda, P. Lošťák, J. Horák, W. Chen, C. Uher, J. Appl. Phys. 94 (2003) 7631.
[8] P. Lošťák, R. Novotný, L. Beneš, S. Civiš, J. Crys. Growth 94 (1989) 656.
[9] M. Stordeur, G. Simon, Phys. Stat. Sol. B 124 (1984) 799.
[10] H. Krebs, Grundzüge der Anorganischen Kristallchemie, F. Enke-Verlag, Stuttgart, 1968, p. 239.
[11] J. Horák, M. Matyáš, L. Tichý, Phys. Stat. Sol. 27 (1975) 621.
[12] G. Offergeld, J. van Cakenberghe, J. Phys. Chem. Solids 11 (1959) 310.
[13] P. Pecheur, G. Toussaint, J. Phys. Chem. Solids 55 (1994) 327.
[14] N. Frangis, S. Kuypers, C. Manolikas, J. van Landuyt, S. Amelinckx, J. Solid State Chem. 69 (1990) 817.
[15] P. Švanda, P. Lošťák, J. Horák, W. Chen, J. S. Dyck, C. Uher, 2002. Seventh European Workshop on Thermoelectrics, Pamplona, October 2002, p. 21.